

# Circularly polarized light in the single-cycle limit: the nature of highly polychromatic radiation of defined polarization

Jie Shan,<sup>1</sup> Jerry I. Dadap,<sup>2</sup> and Tony F. Heinz<sup>3</sup>

<sup>1</sup> Department of Physics, Case Western Reserve University, Cleveland, Ohio 44106, USA

<sup>2</sup> Department of Applied Physics and Applied Mathematics, Columbia University, New York, New York 10027, USA

<sup>3</sup> Departments of Physics and Electrical Engineering, Columbia University, New York, New York 10027, USA

[jie.shan@case.edu](mailto:jie.shan@case.edu), [dadap@phys.columbia.edu](mailto:dadap@phys.columbia.edu), [tony.heinz@columbia.edu](mailto:tony.heinz@columbia.edu)

**Abstract:** We have developed a general analytic description of polarized light pulses and explored the properties of circularly polarized single-cycle pulses. The temporal evolution of the electric-field vector of such spectrally broad pulses, which may be described in terms of a Hilbert transform relationship, differs significantly from the well-known behavior of quasi-monochromatic radiation. Single-cycle circularly polarized pulses have been produced and characterized experimentally in the terahertz spectral region.

©2009 Optical Society of America

**OCIS codes:** (260.5430) Polarization; (300.6495) Spectroscopy, terahertz; (320.0320) Ultrafast optics.

---

## References and links

1. M. Born and E. Wolf, *Principles of Optics: Electromagnetic Theory of Propagation, Interference and Diffraction of Light*, 7 ed. (Cambridge Univ. Press, 1999).
2. S. Huard, *Polarization of Light* (Wiley, New York, 1997).
3. E. Collett, *Polarized Light: Fundamentals and Applications* (Marcel Dekker, New York, 1993).
4. D. Grischkowsky, in *Frontiers in Nonlinear Optics*, H. Walther, N. Koroteev, and M. O. Scully Eds. (Institute of Physics, Philadelphia, 1992), pp. 196-227.
5. G. Steinmeyer, D. H. Sutter, L. Gallmann, N. Matuschek, and U. Keller, "Frontiers in ultrashort pulse generation: Pushing the limits in linear and nonlinear optics," *Science* **286**, 1507-1512 (1999).
6. U. Keller, "Recent developments in compact ultrafast lasers," *Nature* **424**, 831-838 (2003).
7. G. Sansone, E. Benedetti, F. Calegari, C. Vozzi, L. Avaldi, R. Flammini, L. Poletto, P. Villoresi, C. Altucci, R. Velotta, S. Stagira, S. De Silvestri, and M. Nisoli, "Isolated single-cycle attosecond pulses," *Science* **314**, 443-446 (2006).
8. R. A. Cheville, R. W. McGowan, and D. Grischkowsky, "Time resolved measurements which isolate the mechanisms responsible for terahertz glory scattering from dielectric spheres," *Phys. Rev. Lett.* **80**, 269-272 (1998).
9. A. Nahata and T. F. Heinz, "Reshaping of freely propagating terahertz pulses by diffraction," *IEEE J. Sel. Top. Quantum Electron.* **2**, 701-708 (1996).
10. J. Bromage, S. Radic, G. P. Agrawal, C. R. Stroud, P. M. Fauchet, and R. Sobolewski, "Spatiotemporal shaping of half-cycle terahertz pulses by diffraction through conductive apertures of finite thickness," *J. Opt. Soc. Am. B* **15**, 1399-1405 (1998).
11. K. P. Cheung and D. H. Auston, "Distortion of ultrashort pulses on total internal-reflection," *Opt. Lett.* **10**, 218-219 (1985).
12. S. R. Keiding and D. Grischkowsky, "Measurements of the phase-shift and reshaping of terahertz pulses due to total internal-reflection," *Opt. Lett.* **15**, 48-50 (1990).
13. G. Gallot, S. P. Jamison, R. W. McGowan, and D. Grischkowsky, "Terahertz waveguides," *J. Opt. Soc. Am. B* **17**, 851-863 (2000).
14. K. L. Wang and D. M. Mittleman, "Metal wires for terahertz wave guiding," *Nature* **432**, 376-379 (2004).
15. A. B. Ruffin, J. V. Rudd, J. F. Whitaker, S. Feng, and H. G. Winful, "Direct observation of the Gouy phase shift with single-cycle terahertz pulses," *Phys. Rev. Lett.* **83**, 3410-3413 (1999).
16. Q. Chen and X. C. Zhang, "Polarization modulation in optoelectronic generation and detection of terahertz beams," *Appl. Phys. Lett.* **74**, 3435-3437 (1999).

17. R. Shimano, H. Nishimura, and T. Sato, "Frequency tunable circular polarization control of terahertz radiation," *Jpn. J. Appl. Phys.* **44**, L676-L678 (2005).
18. N. Amer, W. C. Hurlbut, B. J. Norton, Y. S. Lee, and T. B. Norris, "Generation of terahertz pulses with arbitrary elliptical polarization," *Appl. Phys. Lett.* **87**, 221111 (2005).
19. Y. Hirota, R. Hattori, M. Tani, and M. Hangyo, "Polarization modulation of terahertz electromagnetic radiation by four-contact photoconductive antenna," *Opt. Express* **14**, 4486-4493 (2006), <http://www.opticsinfobase.org/oe/abstract.cfm?URI=oe-14-10-4486>.
20. N. Kanda, K. Konishi, and M. Kuwata-Gonokami, "Terahertz wave polarization rotation with double layered metal grating of complimentary chiral patterns," *Opt. Express* **15**, 11117-11125 (2007), <http://www.opticsinfobase.org/oe/abstract.cfm?URI=oe-15-18-11117>.
21. J. B. Masson and G. Gallot, "Terahertz achromatic quarter-wave plate," *Opt. Lett.* **31**, 265-267 (2006).
22. The definition of polarized radiation introduced in this paper may be extended to statistical fields through the use of the coherence matrix. The criterion for a fully polarized field is then, in the terminology of Born and Wolf [1], that the complex degree of coherence of the two field components at zero time delay attains its maximum value,  $|\gamma_{xy}(\tau=0)| = 1$ . This criterion also constitutes the natural generalization of existing treatment of quasi-monochromatic radiation.
23. L. Mandel and E. Wolf, *Introduction to the Theory of Fourier Integrals* (Cambridge Univ. Press, Cambridge, New York, 1995).
24. The complex parameter  $\zeta = e_y / e_x$  can be related to the standard parameters of the polarization ellipse. If we denote the angle of the azimuth of the major axis by  $\alpha$  and the ellipticity parameter by  $\xi$ , then  $\zeta = (\tan \alpha + i \tan \xi) / (1 - i \tan \alpha \tan \xi)$ .
25. A. Nahata, A. S. Weling, and T. F. Heinz, "A wideband coherent terahertz spectroscopy system using optical rectification and electro-optic sampling," *Appl. Phys. Lett.* **69**, 2321-2323 (1996).
26. L. A. Nafie, "Infrared and Raman vibrational optical activity: Theoretical and experimental aspects," *Annu. Rev. Phys. Chem.* **48**, 357-386 (1997).
27. S. Spielman, B. Parks, J. Orenstein, D. T. Nemeth, F. Ludwig, J. Clarke, P. Merchant, and D. J. Lew, "Observation of the quasi-particle Hall-effect in superconducting  $\text{YBa}_2\text{Cu}_3\text{O}_{7-\delta}$ ," *Phys. Rev. Lett.* **73**, 1537-1540 (1994).
28. T. J. Binsky, G. Haefliger, and R. R. Jones, "Ionization of Na Rydberg atoms by subpicosecond quarter-cycle circularly polarized pulses," *Phys. Rev. Lett.* **79**, 2018-2021 (1997).
29. D. J. Jones, S. A. Diddams, J. K. Ranka, A. Stentz, R. S. Windeler, J. L. Hall, and S. T. Cundiff, "Carrier-envelope phase control of femtosecond mode-locked lasers and direct optical frequency synthesis," *Science* **288**, 635-639 (2000).
30. A. Baltuska, T. Udem, M. Uiberacker, M. Hentschel, E. Goulielmakis, C. Gohle, R. Holzwarth, V. S. Yakovlev, A. Scrinzi, T. W. Hansch, and F. Krausz, "Attosecond control of electronic processes by intense light fields," *Nature* **421**, 611-615 (2003).
31. E. Gagnon, I. Thomann, A. Paul, A. L. Lytle, S. Backus, M. M. Murnane, H. C. Kapteyn, and A. S. Sandhu, "Long-term carrier-envelope phase stability from a grating-based, chirped pulse amplifier," *Opt. Lett.* **31**, 1866-1868 (2006).

## 1. Introduction

Polarization phenomena occupy a central position in our understanding and application of electromagnetic radiation across its entire spectral range. The polarization properties of quasi-monochromatic radiation have been thoroughly investigated. Various representations of fully and partially polarized quasi-monochromatic radiation, including Jones vectors, Stokes vectors, the Poincaré sphere, and coherence matrices, have been introduced [1,2,3]. For deterministic waves, the polarization state manifests itself in the time domain simply as the form of the elliptical trajectory executed by the electric-field vector of the electromagnetic wave. In this paper we address the question of how to extend this description of polarized light to encompass the general case of *highly polychromatic radiation*. In addition to the intrinsic interest in this fundamental issue, rigorous understanding is critical for the burgeoning applications of electromagnetic radiation in the single or near-single cycle limit. Such radiation can now be produced by laser-based techniques from the terahertz to soft x-ray regions of the spectrum [4,5,6,7]. Here we present a general theoretical description of the temporal evolution of radiation of defined polarization that is valid for light of arbitrary bandwidth and consider its implications for circularly polarized (CP) single-cycle pulses. The behavior, which differs dramatically from the quasi-monochromatic limit of a circular electric-field trajectory, is described by a Hilbert transform relation between the orthogonal

electric-field components. We verify these results experimentally using pulsed terahertz radiation.

The experimental component of the present study relies on the capabilities of terahertz (THz) time-domain spectroscopy [4]. This method permits generation of highly controlled single-cycle pulses of propagating electromagnetic radiation of sufficiently short wavelength to apply optical techniques for polarization control. In addition, the approach permits precise and direct measurement of the magnitude and direction of the electric-field vector as a function of time. These attributes render THz time-domain spectroscopy highly suitable for investigations of fundamental aspects of electromagnetic radiation and wave propagation. Researchers have exploited these capabilities to examine basic aspects of electromagnetic theory that include scattering [8], diffraction [9,10], and other wave-propagation effects, such as total-internal reflection [11,12], wave guiding [13,14], and the Gouy phase shift [15]. Polarization control has also been investigated [16,17,18,19,20] and achromatic polarization control over a large bandwidth has been shown based on total-reflection prisms [19] and a large number of stacked birefringent crystals [21]. In the present investigation, we produce and characterize single-cycle pulses of circularly polarized radiation that are obtained by a rigorous procedure from linearly polarized pulses using an achromatic Fresnel rhomb as a broad-band circular polarizer. The temporal evolution of the resulting electric-field vector is measured by electro-optic sampling to provide a precise determination of the character of CP pulses of single-cycle duration.

## 2. Theoretical description

In order to develop a description of polarized polychromatic radiation, let us first consider a monochromatic plane wave propagating along the  $z$ -axis with the electric field  $\vec{E}(t)$  given by

$$\vec{E}(t) = E_x(t)\hat{x} + E_y(t)\hat{y} = \text{Re}\{\hat{e}E(\omega)e^{-i\omega t}\} \quad (1)$$

as observed at position  $z = 0$ . Here  $\omega$  denotes its angular frequency,  $E(\omega)$  its amplitude, and  $\hat{e}$  its polarization state (where  $\hat{e} \cdot \hat{e}^* = 1$ ). The polarization of such a field is, of course, fully characterized by the unit vector  $\hat{e}$ , with  $\hat{e} = \hat{e}_{\pm} = (\hat{x} \pm i\hat{y})/\sqrt{2}$  representing, left (–) and right (+) CP states. We may then generalize the description to an arbitrary electromagnetic pulse  $\vec{E}(t)$  (with a spatially uniform wavefront) through its Fourier transform representation:

$$\vec{E}(t) = \text{Re} \int_0^{\infty} d\omega \hat{e}(\omega) E(\omega) e^{-i\omega t} . \quad (2)$$

We define this field to be fully polarized if and only if  $\hat{e}(\omega) = \hat{e}$  for all frequencies  $\omega$ . Note that when the radiation in question is quasi-monochromatic in character, this definition is identical to several equivalent formulations of fully polarized quasi-monochromatic radiation applied to deterministic (non-statistical) fields [22]. The present definition is, however, broader: It may be applied to radiation of arbitrary spectral bandwidth.

For the case of fully polarized pulses, Eq. (2) may be rewritten as

$$\vec{E}(t) = \text{Re}\{\hat{e}\tilde{E}(t)\}, \quad (3)$$

where

$$\tilde{E}(t) = \int_0^{\infty} d\omega E(\omega) e^{-i\omega t} \quad (4)$$

is called the analytic signal belonging to its real part,  $E(t)$  [23]. For sufficiently regular functions, the real and imaginary parts of the analytic signal  $\tilde{E}(t)$  are related to one another by Hilbert transforms. The well-known Kramers-Krönig relations for the real and imaginary parts of material response functions are frequency-domain analogs of this Hilbert-transform relationship. While the physical origin of the Kramers-Krönig relations is entirely different from that for the time-domain relations of the two vector components of polarized light, the relations stem mathematically from the same property, namely, that the corresponding Fourier transforms are zero for negative values of their arguments. Making use of the properties of  $\tilde{E}(t)$ , we obtain a direct relation between the two orthogonal Cartesian components of the electric field for pulses of any specified polarization state: Each field component is uniquely determined by knowledge of the temporal evolution of the other, i.e., the trajectory of the full electric-field vector is specified by the waveform of either of its Cartesian components.

To express this relationship explicitly, we assume without loss of generality that  $e_x \neq 0$  and write the polarization state of the field in terms of complex parameter  $\zeta \equiv e_y/e_x = \zeta' + i\zeta''$  [24]. We then obtain the following time-domain description of the fully polarized radiation:

$$\begin{aligned} E_x(t) &= (\zeta' E_y(t) + \zeta'' \text{H}[E_y(t')]) / |\zeta|^2, \\ E_y(t) &= \zeta' E_x(t) - \zeta'' \text{H}[E_x(t')] \end{aligned} \quad (5)$$

where H stands for the Hilbert transformation

$$\text{H}[f(t')] = \frac{1}{\pi} \text{PV} \int_{-\infty}^{\infty} \frac{f(t') dt'}{t' - t}, \quad (6)$$

with PV denoting the Cauchy principal value at  $t = t'$ . For CP pulses, Eq. (5) reduces to

$$\begin{aligned} E_x(t) &= \mp \text{H}[E_y(t')] \\ E_y(t) &= \pm \text{H}[E_x(t')] \end{aligned} \quad (7)$$

with the upper and lower signs corresponding, respectively, to the left and right CP states.

### 3. Nature of circularly polarized short pulses

To examine the nature of CP radiation of differing bandwidth, we write the  $x$ -component of a CP pulse in the form of

$$E_x(t) = |\varepsilon(t)| \sin[\omega_0 t + \varphi(t)] \quad (8)$$

with an envelope function

$$\varepsilon(t) = |\varepsilon(t)| e^{i\varphi(t)} \quad (9)$$

and a mean frequency  $\omega_0$ . Let us first consider quasi-monochromatic radiation where the bandwidth  $\Delta\omega$  of the field is small compared to the mean frequency  $\omega_0$ . For left CP radiation, the  $y$ -component of the electric field for the indicated  $x$ -component is then obtained simply by shifting the phase of each frequency component by  $-\pi/2$ , which yields

$$E_y(t) \approx -|\varepsilon(t)| \cos(\omega_0 t + \varphi(t)). \quad (10)$$

This well-known behavior for CP quasi-monochromatic light follows directly from evaluation of the Hilbert-transform relation of Eq. (7) in the relevant limit of quasi-monochromatic

radiation. In this case, the electric-field vector  $\vec{E}(t)$  rotates with a slowly varying angular speed (or instantaneous frequency) of

$$\dot{\theta}(t) = \omega_0 + \dot{\phi}(t) \quad (11)$$

and a slowly varying amplitude of  $|\varepsilon(t)|$ . If  $\varepsilon(t)$  is real (for an unchirped or transform-limited pulse), then we have simply a constant rotational speed of  $\dot{\theta}(t) = \omega_0$ . This situation is shown in Fig. 1(a).

To illustrate the properties of CP radiation in the strongly polychromatic regime ( $\Delta\omega \sim \omega_0$ ), we consider a transform-limited Gaussian pulse of duration  $\tau$  and amplitude  $E_0$ . From this initial waveform, we can create, for instance, left CP radiation by applying an ideal circular polarizer for which the  $x$ -component of the pulse is unchanged and the  $y$ -component experiences the appropriate phase shift. We thus write

$$E_x(t) = E_0 \exp(-t^2 / \tau^2) \sin(\omega_0 t) \quad (12)$$

and compute the  $y$ -component of the electric field using the Hilbert transform of Eq. (7) on Eq. (12). The corresponding angular speed with which the electric-field vector rotates can be evaluated through the expression

$$\dot{\theta}(t) = [\dot{E}_y(t)E_x(t) - E_y(t)\dot{E}_x(t)]/[E_x^2(t) + E_y^2(t)]. \quad (13)$$

The results for representative pulses with  $\omega_0\tau = 60, 3.5$ , and  $2$  are shown in Fig. 1.

The actual behavior is found to deviate appreciably from the prediction for quasi-monochromatic radiation shown in Fig. 1(a) for pulses with duration  $\tau \sim \omega_0^{-1}$ . Two examples are shown in Figs. 1(b) and 1(c). The choice of  $\tau = 3.5\omega_0^{-1}$  is made to simulate the single-cycle THz pulses generated in the experiment described below, while the lower value of  $\tau = 2\omega_0^{-1}$  exemplifies the distinctive characteristics of highly polychromatic radiation. In both instances, the short duration of the pulse explains the restricted trajectories of the parametric representation of  $\vec{E}(t)$  in Figs. 1(b) and 1(c), which contrast with the usual circular trajectory of a monochromatic wave and the slowly converging or diverging spiral trajectory of a quasi-monochromatic wave [Fig. 1(a)].

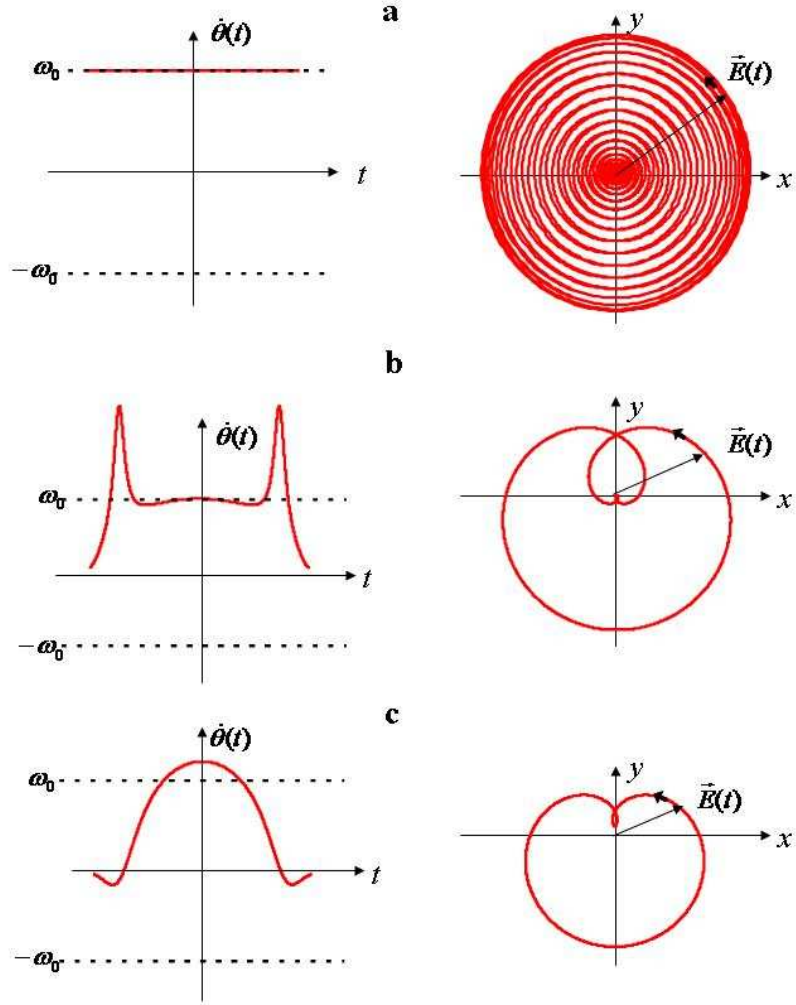


Fig. 1. Right column: Parametric plots of the electric-field vector  $\vec{E}(t)$  of left CP pulses with  $x$ -components given by  $E_x(t) = E_0 \exp(-t^2/\tau^2) \sin(\omega_0 t)$  and the corresponding  $E_y(t)$  calculated by the Hilbert transform of Eq. (7). Panels (a), (b), and (c) correspond to decreasing normalized pulse durations of  $\omega_0 \tau = 60, 3.5,$  and  $2,$  respectively. Left column: Time dependence of the angular speed  $\dot{\theta}(t)$  of the electric-field vector  $\vec{E}(t)$  for the corresponding pulses, plotted for times when the field amplitude exceeds 0.1% of its peak values.

The distinctive properties of the short pulses are highlighted in the time dependence of the instantaneous angular speed  $\dot{\theta}(t)$  of the electric-field vectors  $\vec{E}(t)$ , as shown on the left side of Fig. 1. For both short pulses,  $\dot{\theta}(t)$  deviates markedly from the value  $\omega_0$ , especially at the wings of the pulses, where it may assume a value either well above or below  $\omega_0$ . More remarkably, we also see  $\dot{\theta}(t) < 0$  in certain regimes. This latter situation corresponds to the field vector  $\vec{E}(t)$  rotating for a period of time in the reverse of the expected direction, i.e., in the sense usually associated with CP radiation of the opposite handedness. The origin of this behavior can be understood as arising from the interference of the out-of-phase motion of the circular orbits of widely varying frequencies. The situation can be analyzed explicitly in a

two-frequency model, which allows one to show that such retrograde motion can be significant only for pulses of large fractional bandwidth.

#### 4. Experiment

For our experiment, we have generated and characterized single-cycle CP pulses in the THz spectral range using the apparatus shown in Fig. 2. It consisted essentially of a polarization-sensitive THz time-domain spectrometer that permitted the generation and measurement of single-cycle electromagnetic pulses. The THz spectrometer employed optical rectification of femtosecond laser pulses in a  $\langle 110 \rangle$  ZnTe crystal for the generation of linearly polarized single-cycle THz pulses. The detection of the THz waveform was accomplished by electro-optic sampling with a time-synchronized femtosecond laser pulse in a second ZnTe crystal. Details of the arrangement have been presented elsewhere [25].

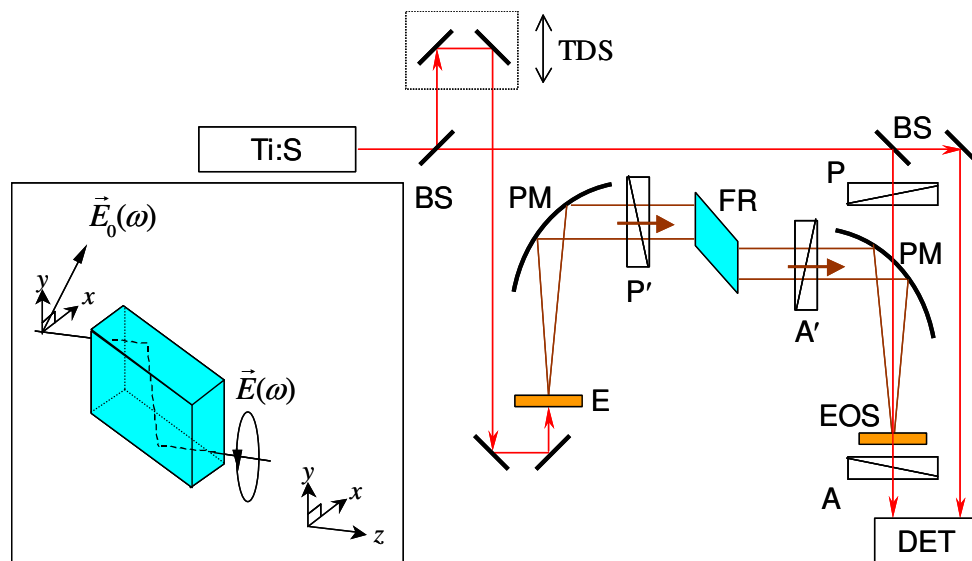


Fig. 2. Experimental setup for the generation of CP THz radiation through the use of a Fresnel rhomb. Ti:Sapphire (Ti:S) laser pulses are split into two beams by a beam splitter (BS). One arm of the beam is delayed using a time-delay stage (TDS), focused into a ZnTe THz emitter (E), collimated by a parabolic mirror (PM) prior to injection into the Fresnel rhomb (FR), and refocused by a second PM into a second ZnTe crystal for electro-optic sampling (EOS) system. The second arm of the laser beam is used for detection in a differential detection (DET) scheme. (P, A) and (P', A') are the polarizer and analyzer for the optical probe and the THz radiation, respectively. The inset is a schematic representation of the Fresnel rhomb arranged to transform linearly polarized pulses to CP pulses.

The key element in the production of the desired CP THz radiation is a Fresnel rhomb shown in the inset of Fig. 2. It was made of high-density polyethylene, a material that is nearly free of loss and dispersion in the THz spectral range (with refractive index  $n = 1.525$ ). The rhomb was designed to function as an achromatic quarter-wave plate, i.e., to introduce a frequency-independent relative phase shift of  $\pi/2$  between orthogonal field components. This relative  $\pi/2$ -phase shift was accomplished through two total internal reflections in the rhomb at an angle of incidence of  $55.7^\circ$ . The Fresnel rhomb then transforms the linearly polarized input radiation arranged to have equal  $s$ - and  $p$ -components into CP radiation. Detection of the polarization characteristics of the resulting radiation is accomplished by recording waveforms for each field component of the THz radiation using the electro-optic sampling technique in conjunction with a wire-grid analyzer (A' in Fig. 2). It should be noted that birefringent

optical elements conventionally employed for polarization control are inherently dispersive, even in the absence of material dispersion, when large fractional bandwidths are considered. Such approaches are thus not suitable for highly polychromatic radiation.

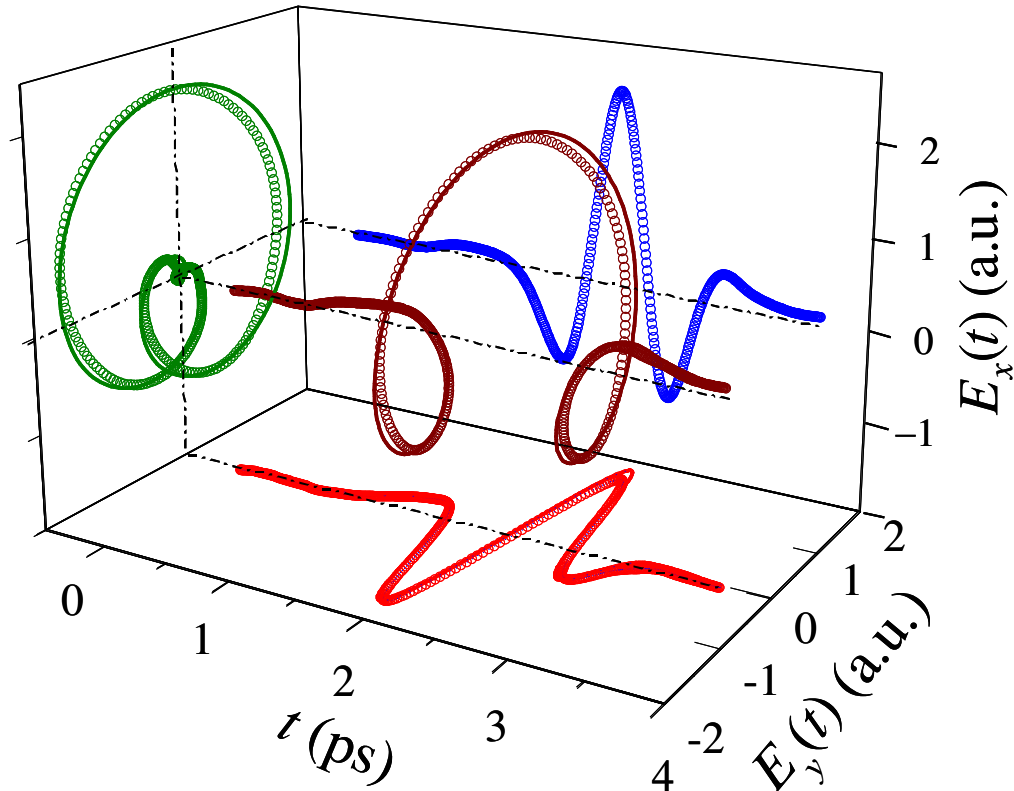


Fig. 3. (a) Time dependence of the electric-field vector, its two orthogonal components  $E_x(t)$  and  $E_y(t)$ , and the parametric plot of the field components for a left CP THz pulse generated in the experiment (symbols). The solid lines correspond to the time dependence of the electric-field vector, the  $y$ -component of which is calculated from the experimental waveform for  $E_x(t)$  by the Hilbert-transform relation of Eq. (7).

Typical time dependence of the electric-field vector for a left CP THz pulse generated in the experiment is shown in a three-dimensional representation in Fig. 3 (symbols). The three projections display waveforms of the two orthogonal field components  $E_x(t)$ ,  $E_y(t)$ , and their parametric plot. The second waveform for the  $y$ -component (solid line) was calculated from the experimental  $x$ -component of the field by the Hilbert transform of Eq. (7). The same data are shown in both the parametric and three-dimensional representations in Fig. 3 as solid lines. The small difference between theory and experiment may reflect inaccuracies in the design of the rhomb, a slight deviation of the angle of incidence from the ideal value or the finite divergence of the THz beam, as phase shifts incurred in total internal reflection depend relatively strongly on angle of incidence. Substantial changes in the instantaneous angular speed  $\dot{\theta}(t)$  of the electric field vector are evident, and retrograde motion of the electric field vector has been observed in some measurements.

## 5. Summary

The goal of this investigation is to provide a rigorous description of circularly polarized short pulses, which should serve to further applications in the THz regime where the time-domain method allows studies of circular dichroism [26] and optical rotary dispersion in diverse physical and chemical systems [27, 28]. The interest in such ultrashort circularly polarized pulses is, however, not confined to the THz spectral range. It extends, for example, to their recent use in the production of high harmonics from circularly polarized optical pulses [7]. The formulation of fully polarized light as comprised of two conjugate components of the electric field that satisfy a Hilbert transform relation, rather than being described simply by a relative phase shift of a carrier wave under a common envelope, may also be relevant in other contexts. In particular, this analysis may bear on recent developments in the optical spectral range where the control of the phase of the electric field of modelocked optical pulses has been achieved [29,30,31].

## Acknowledgments

The authors acknowledge support for this work from the U.S. Air Force Office of Scientific Research and the National Science Foundation under the grant number ECS-05-07111 at Columbia University and under the grant number DMR-0349201 at Case Western Reserve University.